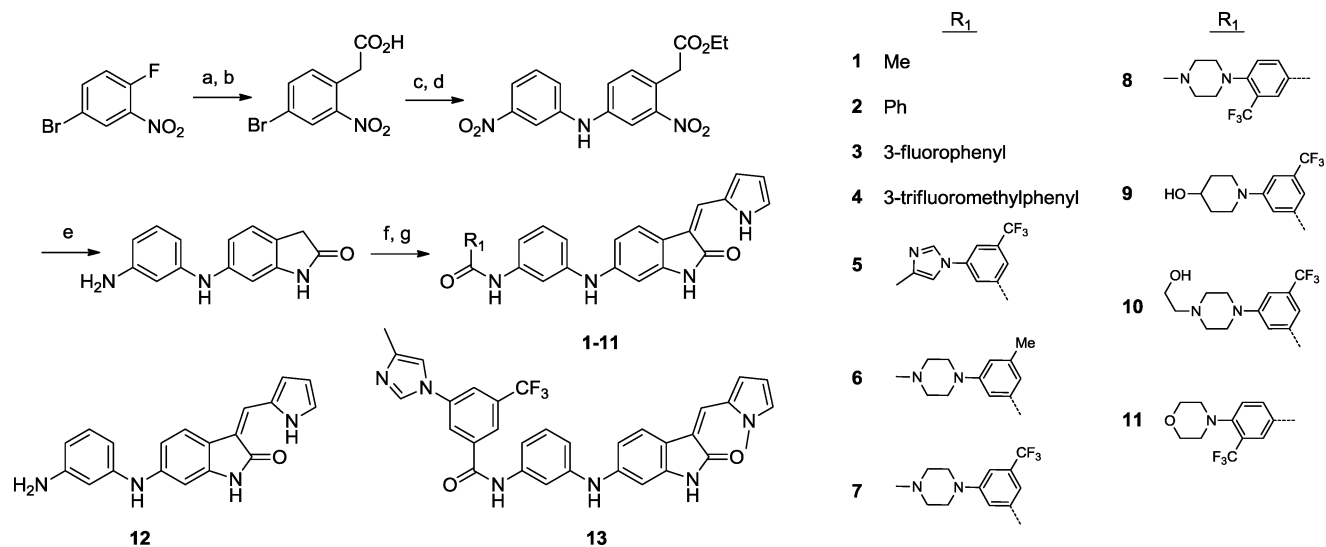


Scheme 1. Preparation of Oxindole Amides 1–11^a

^aReagents and conditions: (a) $\text{CH}_2(\text{CO}_2\text{Me})_2$, NaH, DMSO, 60 °C, 99%. (b) AcOH, HCl, 110 °C, 99%. (c) EtOH, concentrated H_2SO_4 , reflux, 96%. (d) 3-Nitroaniline, $\text{Pd}(\text{OAc})_2$, Xantphos, Cs_2CO_3 , 80 °C, 85%. (e) H_2 (balloon), 10% Pd/C, AcOH, room temperature, 72%. (f) R-COOH, HATU, DIEA, DMF, room temperature, 47–99%. (g) 1H-pyrrole-2-carbaldehyde, EtOH, 80 °C, 35–91%.

Table 1. Cellular and Enzymatic Activities of Oxindole Amides and Ureas

compd	IC_{50} (μM)								
	cellular Ba/F3 assays ^a					biochemical assays ^c			
	TRK			KDR	WT ^b	TRK			
A	B	C	A			B	C		
1	2.3	1.3	1.2	1.0	1.3	NA	NA	1.9	
2	0.91	0.68	0.69	0.60	0.93	0.16	NA	NA	
3	0.85	0.66	0.57	NA	2.2	NA	NA	NA	
4	0.059	0.037	0.023	0.50	4.8	0.007	NA	0.029	
5	0.015	0.005	0.007	0.50	>10	0.007	0.054	NA	
6	0.39	0.22	0.27	2.8	4.7	0.016	NA	0.097	
7	0.013	0.012	0.012	0.50	4.5	0.007	0.007	NA	
8	0.36	0.55	0.44	0.70	2.1	0.027	NA	NA	
9	0.034	0.019	0.029	0.61	4.9	0.003	0.06	NA	
10	0.19	0.079	0.15	4.9	>10	0.068	0.035	NA	
11	0.022	0.020	NA	0.20	4.3	NA	NA	NA	
12	>10	>10	>10	>10	>10	NA	NA	>10	
13	0.36	0.12	0.19	2.2	>10	0.049	NA	NA	
14	0.014	0.005	0.008	0.60	1.3	NA	0.027	NA	
15	>10	>10	>10	>10	>10	NA	NA	NA	
16	0.01	0.003	0.006	1.5	>10	NA	0.017	NA	
17	0.009	0.006	0.022	0.23	5.2	0.004	0.019	NA	
18	0.012	0.004	0.004	1.3	4.6	0.009	NA	NA	
19	0.013	0.011	0.027	NA	1.4	NA	0.015	NA	
20	0.004	0.005	0.004	0.52	2.4	0.007	NA	0.04	
21	0.05	0.017	0.018	3.3	3.3	0.009	NA	NA	
22	0.011	0.009	0.007	3.0	5.6	0.008	0.012	NA	

^aProliferation assays with Tel-TRK or Tel-KDR fusions. ^bProliferation assay using parental Ba/F3 cells. ^cHTRF or Caliper assays with recombinant TRKA, -B, and -C kinase domains.

a significant inhibitory activity only for FMS, KDR, c-Kit, and PDGFR β (Tables 1 and 2).

Medicinal chemistry optimization was initiated with the goal of identifying a compound with increased selectivity over other kinases, especially KDR, and with appropriate physicochemical and pharmacokinetic properties to support in vivo studies. New compounds were tested for antiproliferative effects in Ba/F3-

Tel-TRKA/B/C and Ba/F3-Tel-KDR assays, and the cytotoxicity effects in those assays were compared with effects in parental wild-type Ba/F3 cells (WT). In addition, selected compounds were tested in biochemical assays using either homogeneous time-dependent fluorescence (HTRF) or Caliper method assays with recombinant TRKA, -B, and -C kinase domains (Table 1) to confirm activity.

Table 2. Ba/F3 Cellular Kinase Panel (IC₅₀, μM)

Ba/F3 ^a	4	5	7	16	20	22
ABL ^b	6.4	5.2	3.8	8.2	1.8	8.2
ALK ^c	6.5	5.7	3.0	>10	7.1	6.8
ALK	5.9	5.3	NA	8.8	2.0	3.4
BMX	7.2	6.7	4.9	>10	3.3	6.7
EPHA3	5.2	5.1	NA	5.4	1.9	5.9
EPHB2	2.4	4.5	NA	2.3	1.7	5.8
FGFR3	6.3	7.7	NA	>10	1.7	9.3
FGFR4	5.4	7.0	NA	>10	1.9	7.0
FGR	>10	5.9	NA	6.3	2.0	3.6
FLT1	2.2	>10	3.6	3.2	1.5	4.4
FLT3	9.4	4.7	6.4	5.5	2.1	5.1
FMS	0.31	4.2	3.7	7.6	3.4	4.0
IGF1R	5.6	6.2	5.7	>10	1.5	7.6
INSR	5.8	5.7	5.4	>10	2.9	8.0
JAK2	3.1	5.8	5.1	5.6	1.9	2.9
KIT	0.021	0.013	0.5	0.046	0.13	0.91
MET	9.6	>10	5.1	NA	1.5	5.8
LYN	7.1	6.6	6.0	>10	1.9	7.3
PDGFRβ	0.002	0.1	0.2	NA	0.12	0.87
RET	1.1	0.18	0.8	0.1	1.0	5.3
RON	5.8	>10	4.9	>10	2.7	4.7
ROS	5.5	5.7	6.0	7.0	1.8	6.0
SRC	5.5	5.8	5.3	>10	2.8	7.3
TIE1	7.9	5.4	5.9	7.0	2.9	5.7
ZAP70	4.8	>10	6.0	NA	2.3	4.7

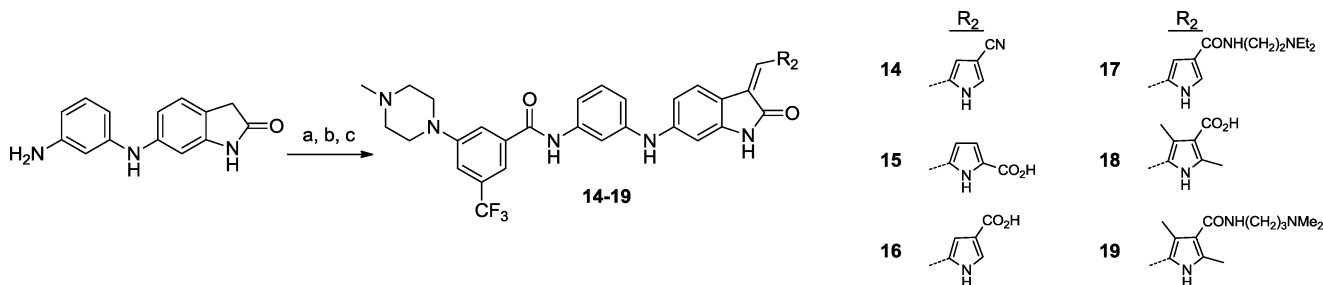
^aBa/F3 cells rendered IL-3 independent by stable transduction with the indicated kinase fused with a Tel dimerization partner unless otherwise specified. ^bBcr-abl. ^cNMP-ALK.

Compounds 1–22 are described in Schemes 1–3. Investigative structure–activity relationship (SAR) of the amide postulated to be occupying the hydrophobic pocket led to the conclusion that the 3-trifluoromethylphenyl-amide is needed to achieve potent cellular TRK inhibitory activity. The unsubstituted benzamide 2 exhibited only very modest activity and replacement of the trifluoromethyl group with a fluorine atom as in 3 led to a decrease in activity. Compound 1, with an acetamide in lieu of a benzamide, exhibited activity similar to that on wild-type cells, indicating loss of specific inhibitory activity for TRK. In an attempt to improve the solubility of the lead compound, the incorporation of heterocyclic groups on the phenyl ring was assessed (5–11). Several basic groups at the 5-position were well tolerated, preferentially in conjunction with the 3-trifluoromethyl group (compare methyl analogue 6

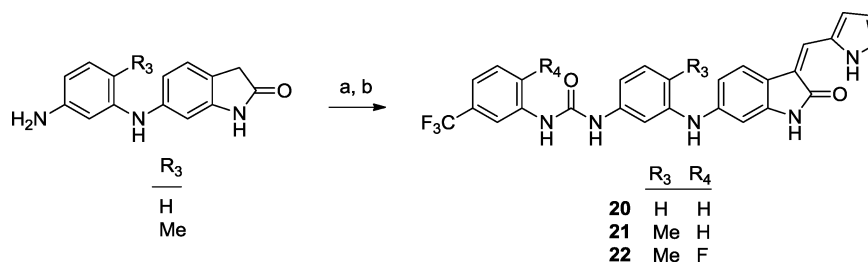
to trifluoromethyl derivative 7). The piperazine at the 4-position led to a drop in activity when compared with the same substitution in the 5-position (8 vs 7). In all cases, the solubility remained low. The elimination of the carbonyl contact to give aniline compound 12 resulted in complete loss of activity as expected for a classic type II DFG-out inhibitor where the amide makes a hydrogen bond contact with the DFG aspartate and glutamate in helix c.²⁶ Replacement of the pyrrole with other groups (pyrrolidine, isooxazole, and cyclopentane) resulted in loss of activity. Methylation of the pyrrole nitrogen of compound 5 yielded a significantly less potent compound (13), suggesting that the pyrrole NH may be involved in a key interaction at the protein hinge region. Decoration on the pyrrole ring led to compounds of varying potency (14–19). The addition of an amide group on the pyrrole at the 4-position (sunitinib like), with or without additional methyl groups, yielded compounds with good potency but poor selectivity against KDR (17 and 19). Excellent potency and selectivity were obtained with the corresponding 4-carboxylic acids (16 and 18). Nitrile replacement of the 4-carboxylic acid (14) was also tolerated, but selectivity was not optimal. In contrast, substitution on the pyrrole with an acid in the 5-position (15) was not tolerated. Replacement of the amide in compound 4 with a urea functionality led to compounds with increased potency and good selectivity against KDR with or without methyl decoration on the central phenyl ring (20 and 21). The addition of a fluorine in the 2-position of the trifluoromethylphenyl ring (22, GNF-5837) further enhanced selectivity over KDR.

Compound 20 was cocrystallized with TRKC and was found to bind to the unactivated kinase (DFG-out) (Figure 1).²⁸ The peptide backbone from the hinge residues E618, Y619, and M620 formed key hydrogen bonds to the heterocycles of 20. A second set of polar interactions involved the compound's urea functionality, which was hydrogen bonded to the side chain of E588 from the α-C-helix and to the peptide backbone of D697 from the DFG motif. The interactions of the urea moiety in this construct were very similar to those documented for other urea derivatives used in kinase inhibitor design.^{29–32} In addition to these polar interactions, two aromatic–aromatic interactions were recognized involving the compound's aminophenyl ring: a stacking interaction with the phenyl ring from the gatekeeper F617 and a face to edge interaction with F698 from the DFG motif.

By virtue of their promising selectivity against KDR, compounds 5, 7, 16, 20, and 22 were tested in a Ba/F3 panel containing 25 additional kinases (Table 2). All of the

Scheme 2. Preparation of Oxindole Amides with Substituted Pyrroles 14–19^a

^aReagents and conditions: (a) 3-(4-Methylpiperazin-1-yl)-5-(trifluoromethyl)benzoic acid, HATU, DIEA, DMF, room temperature, 75%. (b) Corresponding aldehyde, EtOH, 80 °C, 49–80%. (c) Compound 16 to 17 and 18 to 19, corresponding amine, HATU, DIEA, DMF, room temperature, 45–70%.

Scheme 3. Preparation of Oxindole Ureas 20–22^a

^aReagents and conditions: (a) Corresponding isocyanate, TEA, THF, room temperature, 83–94%. (b) 1*H*-pyrrole-2-carbaldehyde, EtOH, 80 °C, 63–87%.

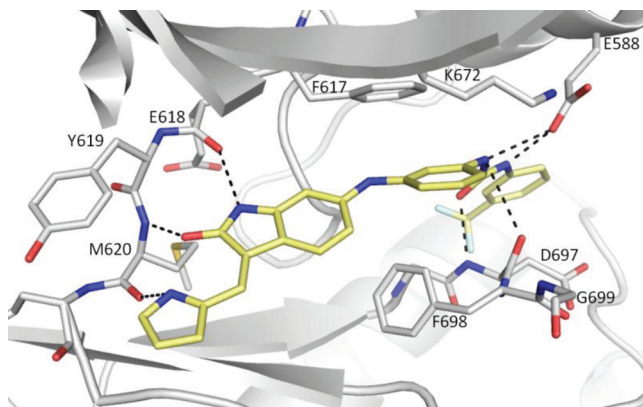


Figure 1. X-ray crystal structure of compound **20** (stick representation; carbon in yellow, oxygen in red, nitrogen in blue, and fluorine in light blue) binding to the active site of TRKC kinase domain. The kinase domain is depicted as a cartoon with carbon atoms in gray, nitrogen in blue, and oxygen in red. Residues of the hinge region, the DFG motif, K672, and E588 are shown as sticks. Hydrogen bonds are shown as dashed lines.

compounds inhibited both *c*-Kit and PDGFR β to varying degrees.

The cellular anti-TRKA activity of compound **22** was further determined in Ba/F3 and RIE (rat intestinal epithelial) cells engineered to express both TRKA and NGF. In Ba/F3 cells expressing TRKA and NGF, **22** demonstrated potent antiproliferation activity with IC₅₀ of 0.042 μ M, whereas it did not have antiproliferative activity up to 10 μ M in parental Ba/F3 cells whose proliferation is dependent on IL-3. RIE cells expressing TRKA and NGF are able to grow and proliferate under low attachment condition and are resistant to detachment-induced apoptosis (anoikis). Compound **22** potently inhibited cell growth and proliferation of RIE cells expressing TRKA and NGF under the low attachment condition with an IC₅₀ of 0.017 μ M.

Inhibitory activities for *c*-Kit and PDGFR were confirmed in cellular assays in Mo7e cells and Rat-A10 cells, respectively. In those assays, compound **22** showed activity in the submicromolar to micromolar range (IC₅₀ Mo7e-*c*-Kit, 1 μ M; IC₅₀ Rat-A10-PDGFR, 0.5 μ M), allowing for a significant selectivity window for TRK over *c*-Kit and PDGFR (IC₅₀RIE-NGF, 0.017 μ M).

To determine the in vivo PK data, compound **22** was administered intravenously to male Balb/c mice and Sprague–Dawley rats, and the drug clearance was found to be low and the volume of distribution moderate (mice) to high (rat). When administered orally by gavage, it gave moderate

bioavailability in both mice and rats due to poor absorption deriving from a combination of poor permeability and low aqueous solubility (Table 3). In the mice, the drug

Table 3. In Vivo PK Properties of Compound **22**

species	Balb/c mice		Sprague–Dawley rats	
	iv	po	iv	po
route ^a				
dose (mg/kg)	5	20	3	10
AUC (h nM)	19339	14293	10616	6837
CL (mL/min/kg)	8.2		9	
V _{ss} (L/kg)	1.4		3.6	
C _{max} (nM)	16360	1173	5196	449
T _{1/2} (h)	4.4	4.5	7.5	7.1
F (%)		18		19

^aFormulated in PEG300:DSW/3:1 as a solution.

concentration in the brain after oral delivery was below the limit of quantitation, suggesting that the compound does not effectively cross the blood–brain barrier.

To demonstrate in vivo efficacy, compound **22** was administered at ascending doses once daily for 10 days in mice (Figure 2) with established tumor xenografts derived from

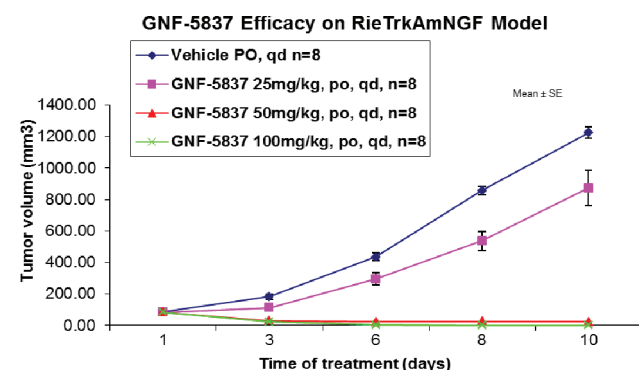


Figure 2. Efficacy of GNF-5837 (**22**) in Rie-TRKAmNGF xenograft model.

RIE cells expressing both TRKA and NGF. In this study, 72 and 100% tumor regression was observed at 50 and 100 mg/kg, respectively. At 25 mg/kg, only partial tumor growth inhibition was achieved.³³

In summary, we have identified a pan TRK inhibitor with excellent selectivity against other kinases, acceptable pharmacokinetic properties, and proven efficacy in vivo. The properties of **22** make it a good tool for the elucidation of TRK biology in cancer and other disease areas. In addition, we have disclosed

the first crystal structure of TRKC with a TRKC inhibitor, which has the potential to aid the design of other classes of selective TRK inhibitors.

■ ASSOCIATED CONTENT

■ Supporting Information

Experimental procedures and characterization of compounds 4, 5, 7, 16, 20, and 22; kinase selectivity and ADMET data for compound 22; and details of in vitro and in vivo assays. This material is available free of charge via the Internet at <http://pubs.acs.org>.

■ AUTHOR INFORMATION

Corresponding Author

*Tel: 858-332-4736. Fax: 858-812-1648. E-mail: vmolteni@gnf.org.

Notes

The authors declare no competing financial interest.

■ ACKNOWLEDGMENTS

We thank Eric Peters and Daniel Mason for HRMS data and David Jones for NMR data.

■ REFERENCES

- (1) Huang, E. J.; Reichardt, L. F. TRK receptors: Roles in neuronal signal transduction. *Annu. Rev. Biochem.* **2003**, *72*, 609–642.
- (2) Pierotti, M. A.; Greco, A. Oncogenic rearrangements of the NTRK1/NGF receptor. *Cancer Lett.* **2006**, *232*, 90–98.
- (3) Lei, L.; Parada, L. F. Transcriptional regulation of TRK family neurotrophin receptors. *Cell. Mol. Life Sci.* **2007**, *64*, 522–532.
- (4) Lagadec, C.; Meignan, S.; Adriaenssens, E.; Foveau, B.; Vanhecke, E.; Romon, R.; Toillon, R. A.; Oxombre, B.; Hondermarck, H.; Le Bourhis, X. TRKA overexpression enhances growth and metastasis of breast cancer cells. *Oncogene* **2009**, *28*, 1960–1970.
- (5) Borrello, M. G.; Bongarzone, I.; Pierotti, M. A.; Luksch, R.; Gasparini, M.; Collini, P.; Pilotti, S.; Rizzetti, M. G.; Mondellini, P.; De Bernardi, B.; Di Martino, D.; Garaventa, A.; Brisigotti, M.; Tonini, G. P. TRK and *ret* proto-oncogene expression in human neuroblastoma specimens: High frequency of TRK expression in non-advanced stages. *Int. J. Cancer* **1993**, *54*, 540–545.
- (6) Ma, J.; Jiang, Y.; Jiang, Y.; Sun, Y.; Zhao, X. Expression of nerve growth factor and tyrosine kinase receptor A and correlation with perineural invasion in pancreatic cancer. *J. Gastroenterol. Hepatol.* **2008**, *23*, 1852–1859.
- (7) Zhu, Z.; Friess, H.; diMola, F. F.; Zimmermann, A.; Graber, H. U.; Korc, M.; Buchler, M. W. Nerve growth factor expression correlates with perineural invasion and pain in human pancreatic cancer. *J. Clin. Oncol.* **1999**, *17*, 2419–2428.
- (8) Festuccia, C.; Muzi, P.; Gravina, G. L.; Millimaggi, D.; Specia, S.; Dolo, V.; Ricevuto, E.; Vicentini, C.; Bologna, M. Tyrosine kinase inhibitor CEP-701 blocks the NTRK1/NGF receptor and limits the invasive capability of prostate cancer cells in vitro. *Int. J. Oncol.* **2007**, *30*, 193–200.
- (9) Davidson, B.; Reich, R.; Lazarovici, P.; Nesland, J. M.; Skrede, M.; Risberg, B.; Trope, C. G.; Florenes, V. A. Expression and activation of the nerve growth factor receptor TRKA in serous ovarian carcinoma. *Clin. Cancer Res.* **2003**, *9*, 2248–2259.
- (10) Thiele, C. J.; Li, Z.; McKee, A. E. On TRK—The TRKB signal transduction pathway is an increasingly important target in cancer biology. *Clin. Cancer Res.* **2009**, *15*, S962–S967.
- (11) Martin-Zanca, D.; Hughes, S. H.; Barbacid, M. A human oncogene formed by the fusion of truncated tropomyosin and protein tyrosine kinase sequences. *Nature* **1986**, *319*, 743–748.
- (12) Butti, M. G.; Bongarzone, I.; Ferraresi, G.; Mondellini, P.; Borrello, M. G.; Pierotti, M. A. A sequence analysis of the genomic regions involved in the rearrangements between TPM3 and NTRK1

genes producing TRK oncogenes in papillary thyroid carcinomas. *Genomics* **1995**, *28*, 15–24.

- (13) Greco, A.; Mariani, C.; Miranda, C.; Pagliardini, S.; Pierotti, M. A. Characterization of the NTRK1 genomic region involved in chromosomal rearrangements generating TRK oncogenes. *Genomics* **1993**, *18*, 397–400.

- (14) Bounacer, A.; Schlumberger, M.; Wicker, R.; Du-Villard, J. A.; Caillou, B.; Sarasin, A.; Suarez, H. G. Search for NTRK1 proto-oncogene rearrangements in human thyroid tumours originated after therapeutic radiation. *Br. J. Cancer* **2000**, *82*, 308–314.

- (15) Beimfohr, C.; Klugbauer, S.; Demidchik, E. P.; Lengfelder, E.; Rabes, H. M. NTRK1 re-arrangement in papillary thyroid carcinomas of children after the Chernobyl reactor accident. *Int. J. Cancer* **1999**, *80*, 842–847.

- (16) Tognon, C.; Knezevich, S. R.; Huntsman, D.; Roskelley, C. D.; Melnyk, N.; Mathers, J. A.; Becker, L.; Carneiro, F.; MacPherson, N.; Horsman, D.; Poremba, C.; Sorensen, P. H. B. Expression of the ETV6-NTRK3 gene fusion as a primary event in human secretory breast carcinoma. *Cancer Cell* **2002**, *2*, 367–376.

- (17) Lannon, C. L.; Sorensen, P. H. B. ETV6-NTRK3: A chimeric protein tyrosine kinase with transformation activity in multiple cell lineages. *Semin. Cancer Biol.* **2005**, *15*, 215–223.

- (18) Watanabe, N.; Kobayashi, H.; Hiramata, T.; Kikuta, A.; Koizumi, S.; Tsuru, T.; Kaneko, Y. Cryptic t(12;15)(p13;q26) producing the ETV6-NTRK3 fusion gene and no loss of IGF2 imprinting in congenital mesoblastic nephroma with trisomy 11 fluorescence in situ hybridization and IGF2 allelic expression analysis. *Cancer Genet. Cytogenet.* **2002**, *136*, 10–16.

- (19) Izbicka, E.; Izbicki, T. Therapeutic strategies for the treatment of neuroblastoma. *Curr. Opin. Invest. Drugs* **2005**, *6*, 1200–1214.

- (20) Douma, S.; Van Laar, T.; Zevenhoven, J.; Meuwissen, R.; Van Garderen, E.; Peeper, D. S. Suppression of anoikis and induction of metastasis by the neurotrophic receptor TRKB. *Nature* **2004**, *430*, 1034–1039.

- (21) Miknyoczki, S. J.; Chang, H.; Klein-Szanto, A.; Dionne, C. A.; Ruggeri, B. A. The TRK tyrosine kinase inhibitor CEP-701 (KT-5555) exhibits significant antitumor efficacy in preclinical xenograft models of human pancreatic ductal adenocarcinoma. *Clin. Cancer Res.* **1999**, *5*, 2205–2212.

- (22) Ketterer, K.; Rao, S.; Friess, H.; Weiss, J.; Buechler, M. W.; Korc, M. Reverse transcription-PCR analysis of laser-captured cells points to potential paracrine and autocrine actions of neurotrophins in pancreatic cancer. *Clin. Cancer Res.* **2003**, *9*, 5127–5136.

- (23) Scwab, G. M.; Fujioka, S.; Schmidt, C.; Li, Z.; Frederick, W. A. I.; Yang, W.; Yokoi, K.; Evans, D. B.; Abbruzzese, J. L.; Hess, K. R.; Zhang, W.; Fidler, I. J.; Chiao, P. Overexpression of tropomyosin-related kinase B in metastatic human pancreatic cancer cells. *Clin. Cancer Res.* **2005**, *11*, 440–449.

- (24) Wang, T.; Yu, D.; Lamb, M. L. TRK kinase inhibitors as new treatments for cancer and pain. *Expert Opin. Ther. Patents* **2009**, *19*, 305–319 and references therein.

- (25) Bouhana, K. S.; Impastato, R.; Pheneger, J.; Jiang, Y.; Wallace, R. D.; Do, M. G.; Zautke, N. A.; Andrews, S. W. Analgesic Effects of a Potent and Selective Kinase Inhibitor of Neurotrophin Receptors TRKA, TRKB and TRKC. www.arraybiopharma.com; WO2010033941; WO2010048314; WO11006074.

- (26) Okram, B.; Nagle, A.; Adrian, F. J.; Lee, C.; Ren, P.; Wang, X.; Sim, T.; Xie, Y.; Wang, X.; Xia, G.; Spraggon, G.; Warmuth, M.; Liu, Yi.; Gray, N. S. A General Strategy for Creating “Inactive-Conformation” Abl Inhibitors. *Chem. Biol.* **2006**, *13*, 779–786.

- (27) Melnick, J. S.; Janes, J.; Kim, S.; Chang, J. Y.; Sipes, D. G.; Gunderson, D.; Jarnes, L.; Matzen, J. T.; Garcia, M. E.; Hood, T. L.; Beigi, R.; Xia, G.; Harig, R. A.; Asatryan, H.; Yan, S. F.; Zhou, Y.; Gu, X. J.; Saadat, A.; Zhou, V.; King, F. J.; Shaw, C. M.; Su, A. I.; Downs, R.; Gray, N. S.; Schultz, P. G.; Warmuth, M.; Caldwell, J. S. An efficient rapid system for profiling the cellular activities of molecular libraries. *Proc. Natl. Acad. Sci. U.S.A.* **2006**, *103*, 3153–3158.

- (28) Structure coordinates have been deposited with the PDB: code 3V5Q.

(29) Dar, A. C.; Lopez, M. S.; Shokat, K. M. Small Molecule Recognition of c-Src via the Imatinib-Binding Conformation. *Chem. Biol.* **2008**, *15*, 1015–1022.

(30) Simard, J. R.; Klueter, S.; Gruetter, C.; Getlik, M.; Rabiller, M.; Rode, H. B.; Rauh, D. A. New screening assay for allosteric inhibitors of cSrc. *Nat. Chem Biol.* **2009**, *5*, 394–396.

(31) Pargellis, C.; Tong, L.; Churchill, L.; Cirillo, P. F.; Gilmore, T.; Graham, A. G.; Grob, P. M.; Hickey, E. R.; Moss, N.; Pav, S.; Regan, J. Inhibition of p38 MAP kinase by utilizing a novel allosteric binding site. *Nat. Struct. Biol.* **2002**, *9*, 268–272.

(32) Wan, P. T. C.; Garnett, M. J.; Roe, S. M.; Lee, S.; Niculescu-Duvaz, D.; Good, V. M.; Jones, C. M.; Marshall, C. J.; Springer, C. J.; Barford, D.; Marais, R. Mechanism of activation of the RAF-ERK signaling pathway by oncogenic mutations of B-RAF. *Cell* **2004**, *116*, 855–867.

(33) PD data for compound **22** (GNF-5837) will be described in detail in a manuscript currently in preparation and to be published elsewhere.